ACS APPLIED MATERIALS & INTERFACES

Research Article

www.acsami.org

# Fabrication of Gold Nanoparticles by Laser Ablation in Liquid and Their Application for Simultaneous Electrochemical Detection of $Cd^{2+}$, $Pb^{2+}$, $Cu^{2+}$, $Hg^{2+}$

Xiaoxia Xu, Guotao Duan,* Yue Li, Guangqiang Liu, Jingjing Wang, Hongwen Zhang, Zhengfei Dai, and Weiping Cai*

Key Lab of Materials Physics, Anhui Key lab of Nanomaterials and Nanotechnology, Institute of Solid State Physics, Chinese Academy of Sciences, Hefei, 230031, Anhui, P. R. China

Supporting Information

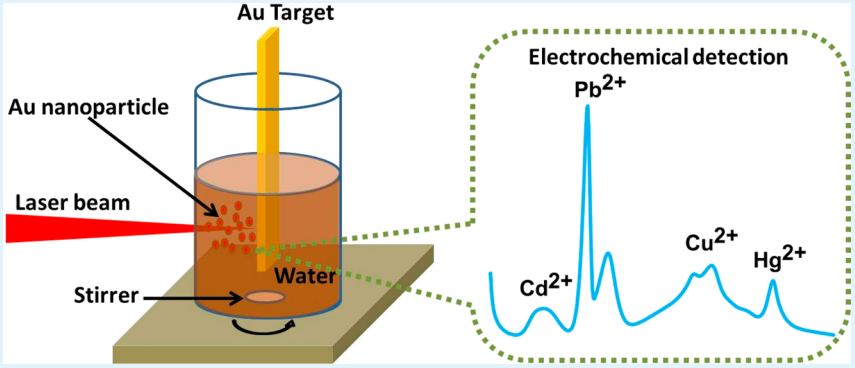


**ABSTRACT:** In this paper, we demonstrated the fabrication of high active and high sensitive Au nanoparticles by laser ablation in liquid (LAL) method, and their application in electrochemical detection of heavy metal ions. First, LAL method are used to fabricate Au nanoparticles in water in a clean way. Second, the Au nanoparticles were assembled onto the surface of the glassy carbon (GC) electrode by an electrophoretic deposition method to form an AuNPs/GC electrode for electrochemical characterization and detection. Through differential pulse anodic stripping voltammetry method, it shows that the AuNPs/GC electrode could be used for the simultaneous and selective electrochemical detection of $Cd^{2+}$, $Pb^{2+}$, $Cu^{2+}$, and $Hg^{2+}$. By studying the influence of test conditions to optimize the electrochemical detection, we can detect $Cd^{2+}$, $Pb^{2+}$, $Cu^{2+}$, and $Hg^{2+}$ simultaneously with a low concentration of $3 \times 10^{-7}$ M in the experiments.

**KEYWORDS:** *laser ablation in liquid, gold nanoparticle, electrochemical detection*

## 1. INTRODUCTION

With the development of industry and agriculture, heavy metal pollution is becoming more and more serious. This kind of contamination by entering the food chain in ecological systems have posed significant hazards to living organisms even at per million concentrations due to their toxicity, accumulation, and low rate of clearance, especially to the health of human beings.[1,2] Recently this phenomenon has aroused wide concern, and precise identification and concentration assessment of heavy metal ions in water or in the soil are increasingly important. So far, a number of techniques and methods have been utilized to detect heavy metal ions, including atomic absorption spectroscopy (AAS).[3] Atomic fluorescence spectrometry (AFS),[4] hyper-Rayleigh scattering,[5] and inductively coupled plasma mass spectrometry (ICP-MS).[6] Although these methods are used widely in laboratory and more successful, they are not suitable for in situ analysis due to the ponderous and complication instruments. In contrast, the electrochemical technique has several advantages over these methods as they are excellently sensitive, simple, fast, and inexpensive. Moreover, its portability and low detection limit permit its use in online trace detection. Among electrochemical methods, electrochemical anodic stripping voltammetry can simultaneously analyze several heavy metal ions.[7−12] Up to now, anodic stripping voltammetry have been widely used in determination of heavy metals in liquid, among which differential pulse anodic stripping voltammetry (DPASV) is especially adopted due to its enhanced faradaic current and decreased nonfaradaic charging current.[13−18]

Obviously, electrode materials are crucial for electrochemical detection performance. Compared to the traditional electrodes materials, nanostructured materials have received great interests due to their enhanced electrochemical performances.[19,20] Electrochemical sensors using nanomaterials mainly take

Received: June 25, 2013
Accepted: December 10, 2013
Published: December 10, 2013

   dx.doi.org/10.1021/am404816e | ACS Appl. Mater. Interfaces 2014, 6, 65−71

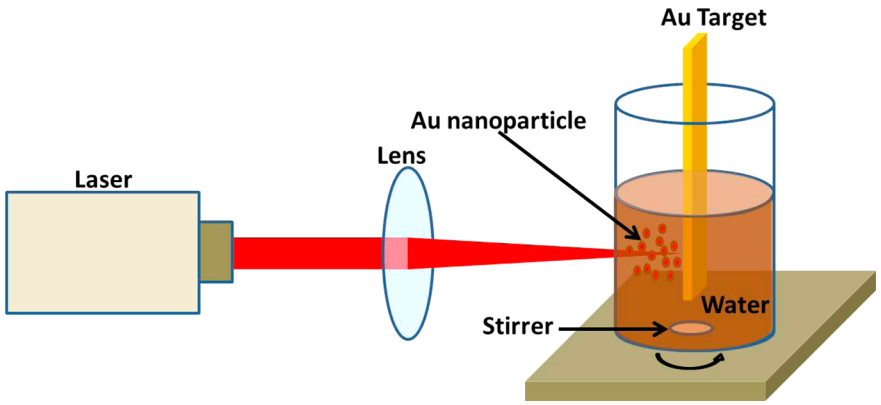


**Figure 1.** Schematic illustration of laser ablating gold target in water.

advantage of their large surface area, fast electronic transport properties, and high electrocatalytic activities.[21,22] Many heavy metal sensors based on the use of carbon nanostructured materials,[23,24] mesoporous silica,[25] and modifications using nanoparticles, such as silver,[26] bismuth,[27] and gold nanoparticles,[7,13,28,29] have been reported. Gold nanoparticles are widely used in chemical and biological sensors due to their highly stability, unique optoelectronic properties, excellent biocompatibility, and so on.[30] A lot of preparative methods for gold nanoparticles have been reported, but they mainly focus on the "bottom-up" chemical approaches. On the basis of our former work on laser ablation in liquid (LAL),[31−35] we prepared the gold nanoparticles by a "top-down" method.

In the past years, LAL has proven to be an effective method for the formation of nanocrystals for different materials, such as, metals (Au, Ag, Pt, Cu, Co),[36−41] semiconductors (Si, ZnO, $TiO_2$, $GeO_2$, etc),[42−47] and diamond and related nanocrystals (diamond, c-BN, $C_3N_4$).[48−50] Unlike other synthetic technique of nanomaterials, the LAL is a very fast and far-from equilibrium process, in which the plasma plume from laser ablation in liquid is in the high-temperature, high-pressures state and contains highly excited high-density radicals from target and solution with high kinetic energy. Therefore, LAL has become an important method to prepare nanostructured materials with metastable phases[51] and immiscible alloying phase.[52] In addition, compared to conventional chemical methods, the technique of LAL is a chemically "simple and clean" synthesis strategy because no catalysts and surfactants are used in the process. Thus, a major advantage of LAL is that the as-fabricated nanomaterials have bare surfaces with higher activity. Therefore, we used the high active and high sensitive Au nanoparticles prepared by LAL in electrochemical detection of heavy metal ions. The details are as follows.

## 2. EXPERIMENTAL SECTION

**2.1. Chemical Reagents.** All reagents were obtained from Alfa Aesar Corporation with analytical grade and were used without further purification. Standard mixed metal ion solutions of $10^{-5}$ mol/L were prepared and stepwise diluted to corresponding solubility immediately before use. All solutions and subsequent dilutions were prepared using deionized water purified by Milli-Q filtration system (Millipore, Japan) with a resistivity of not less than 18 MΩ·cm. Acetate buffer solutions were prepared by adjusting stock solutions of 0.1 M sodium acetate (NaAc) to different pH by adding 0.1 M acetic acid (HAc). The dissolved oxygen in water was removed by purging solutions with high-purity argon for 1 h prior to each measurement.

**2.2. Preparation of Au Colloid.** Au colloidal solution was prepared through pulsed laser ablation of a gold plate (99.99%) which is immersed in deionized water at room temperature. The gold plate was fixed on the bracket in a glass vessel filled with 10 mL deionized water which was continuously stirred during irradiating. The laser was first harmonic 1064 nm Nd:YAG, operated at 60 mJ/pulse with a pulse duration of 10 ns and a frequency of 10 Hz. The laser beam was focused on the gold target with a 2 mm spot size in diameter through a lens with a focal length of 150 mm for 30 min. The solution gradually became red with the increase of ablation time. Au colloidal solution was obtained.

**2.3. Preparation of Au Nanoparticles-Modified GC Electrode (AuNPs/GCE) by Electrophoretic Deposition.** Prior to the surface modification, the bare glassy carbon electrode (diameter 2.0 mm) was abraded with fine SiC paper, polished carefully with 1.0, 0.3, and 0.05 μm alumina slurry, and then, sonicated in 10% nitric acid, ethanol, and deionized water successively to clean the surface and remove any polishing residue. Finally, bare glassy carbon electrode (GCE) was dried under nitrogen flow. Subsequently, we started to functionalize the bare GCE by electrophoretic deposition of Au NPs onto its surface. The cleaned GCE and platinum wire electrode were used as anode and cathode electrodes under a potential of 1.0 V for 90 min immersed in the as-prepared Au colloidal solution (about 10 mL). The distance between the two electrodes was maintained at 8 mm. The bare GCE could be successfully modified by the Au nanoparticles, because the Au nanoparticles obtained by laser ablation in water are negatively charged with the zeta potential of −58.8 mV. After electrophoresis, the AuNPs/GC electrode was rinsed softly by deionized water and then dried by nitrogen flow. Before testing, the AuNPs/GC electrode was activated in 0.5 mol/L sulphuric acid using cyclic voltammetry in order to improve its sensitivity. The potential scan was performed from −1.0 to 1.0 V vs Ag/AgCl with scan rate of 50 mV/s until the curve was stable.

**2.4. $Cd^{2+}$, $Pb^{2+}$, $Cu^{2+}$, and $Hg^{2+}$ Detection.** Differential pulse anodic stripping voltammetry was used for the detection under optimized conditions. First, Cd, Pb, Cu, and Hg were deposited at the potential of −1.0 V vs Ag/AgCl (saturated KCl) for 300 s by the reduction of $Cd^{2+}$, $Pb^{2+}$, $Cu^{2+}$, and $Hg^{2+}$ in 0.1 M NaAc-HAc (pH 5.0). Then, these metals were stripped to metal ions by anodic oxidation under the following experimental conditions: potential range of −1.0 to 0.5 V; increment potential = 4 mV; amplitude = 50 mV; pulse width =


dx.doi.org/10.1021/am404816e | ACS Appl. Mater. Interfaces 2014, 6, 65−71

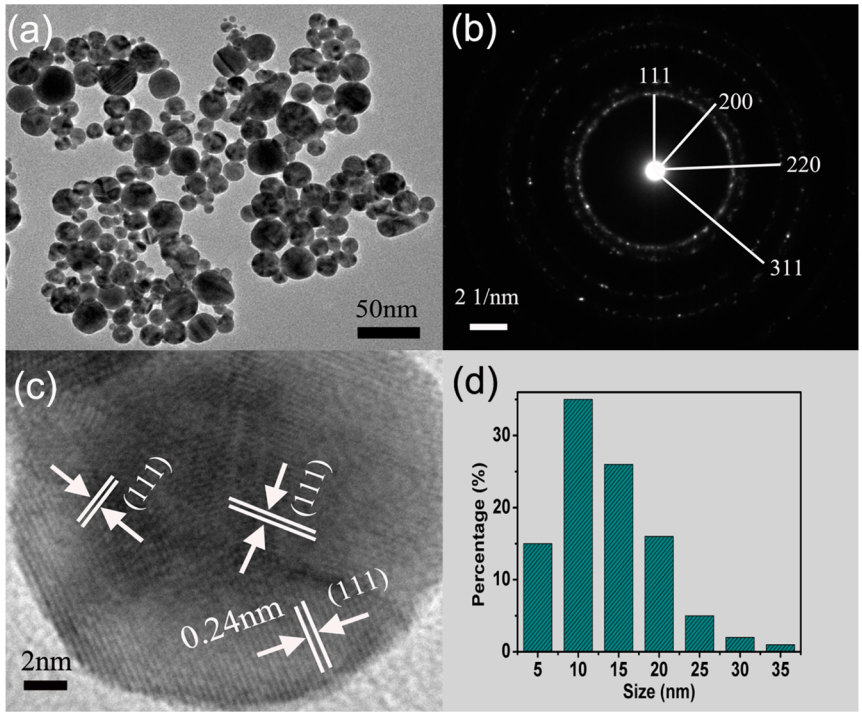


**Figure 2.** (a) TEM images of Au nanoparticles in the colloidal solution formed by laser ablation of Au terget in water. (b–d) Corresponding SAED patterns, typical HRTEM image, and particle size distribution of Au nanoparticles in part a, respectively.

0.06 s. The simultaneous detection of $Cd^{2+}$, $Pb^{2+}$, $Cu^{2+}$, and $Hg^{2+}$ has been performed at the same experimental condition. At the end of each detection test, applying a 1 V potential on the working electrode for 100 s in order to remove the deposited residual species from its surface.

**2.5. Apparatus.** Electrochemical experiments were recorded using a CHI 660C computer-controlled potentiostat (ChenHua Instruments Co., Shanghai, China) with a standard three-electrode system. A bare glassy carbon electrode (GCE, diameter of 2 mm) or modified GCE served as a working electrode; a platinum wire was used as a counter-electrode, and an Ag/AgCl (sat'd KCl) electrode was used as reference electrode. Transmission electron microscopy (TEM), high-resolution transmission electron microscopy (HR-TEM), and selected area electron diffraction (SAED) studies were performed on a JEM-200CX operated at 200 kV. The morphologies of the electrode were measured using a field-emission scanning electron microscope (FESEM, Sirion 200).

## 3. RESULTS AND DISCUSSION

**3.1. Morphologic Characterization of Au Nanoparticles.** The LAL process is illustrated in Figure 1. First, the laser beams through the convex lens focus on the gold plate in deionized water. The high-temperature and high-pressure gold plasma is then produced in the solid–liquid interface quickly after the interaction between a pulsed laser and the gold target. After that, the subsequent ultrasonic and adiabatic expansion of the hot Au plasma leads to cooling of the Au plume region and hence formation of Au clusters. Then, with the extinguishment of the plasma, the Au nanoparticles formed.

Figure 2a shows the TEM image of the as-prepared nanoparticles in the colloidal solution. These products are nearly spherical in shape, and the diameter of the nanoparticles is between 5 and 35 nm, as is shown in Figure 2d. The corresponding selected area electron diffraction pattern indicates that the as-prepared nanoparticles are of gold crystals (see Figure 2b). A typical HRTEM image of one Au nanoparticle is shown in Figure 2c. The images show (111) plane of as-prepared Au nanoparticles. It is worthy noticing that the as-prepared nanoparticles contain many ultrafine crystalline Au grains, with many disordered areas surrounding them. This is in similar with our previous results prepared by LAL method, such as ZnO nanoparticles.[53] The as-prepared Au nanoparticles are rich in high concentration of defect, which may be produced in the nonequilibrium process. Because such defects have high energy, the as-prepared gold nanoparticles may have high chemical activity.

**3.2. Electrochemical Characterization of Au NPs/GC Electrode.** In order to get surface and electrochemical active information about the Au nanoparticles modified glassy carbon, we characterized the electrode by FESEM and cyclic voltammogram. A typical FESEM image of Au nanoparticles on glassy carbon was shown in Supporting Information Figure S1. Clearly, scattered and more uniform Au nanoparticles disperse points appeared in the picture. This demonstrated that clean and high active Au nanoparticles by LAL have been successfully modified on the glassy carbon through electrophoresis. The cyclic voltammetric signals of bare and Au nanoparticles modified GCE has been examined in neutral solution of 5 mM $Fe(CN)_6^{3-/4-}$ containing 0.1 M $KNO_3$ (see Figure 3a). Compared with the bare GCE, the anodic and cathodic peak currents of the AuNPs/GC electrode is higher. The increase of peak current can be contributed to the modified Au nanoparticles. This indicated that the rate of electron transfer at the Au NPs/GC electrode has been increased. The Au NPs/GC electrode has better electrochemical catalytic behavior and promotion of electron transfer process at the modified electrode surface.[54] This may be attributed to the high activity of the Au nanoparticles prepared by LAL. Cyclic voltammetric curves of bare and AuNPs/GC


dx.doi.org/10.1021/am404816e | ACS Appl. Mater. Interfaces 2014, 6, 65–71

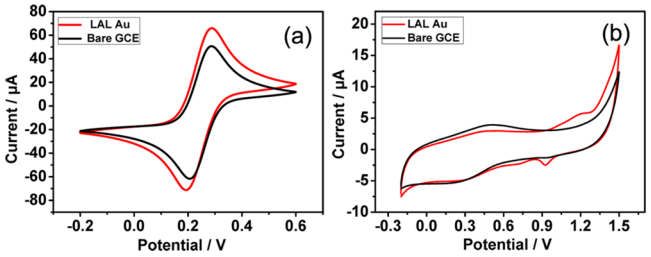


**Figure 3.** Cyclic voltammograms response of bare and Au nanoparticle modified GCE in the solution of 5 mM $Fe(CN)_6^{3-/4-}$ containing 0.1 M $KNO_3$ (a) and in 0.5 M $H_2SO_4$ solution step from −0.2 to 1.5 V vs Ag/AgCl (b).

electrode were recorded in 0.5 M $H_2SO_4$ in the potential range from −0.2 to 1.5 V (vs Ag/AgCl) with the scan rate of 100 mV/s corresponding to black and red line in Figure 3b. We can see that there was no peak in forward or backward scan of bare glassy carbon. However, there appeared a single reduction peak at +0.92 V (vs Ag/AgCl) of Au NPs/GC electrode which due to the reduction of gold surface oxide.[55] According to these CV curves, we deduced the real surface area of the Au nanoparticles on the glassy carbon electrode was about 3.5%.[56]

Figure 4 presents the DPASV analytical characteristics of AuNPs/GC electrode. When the accumulation process was

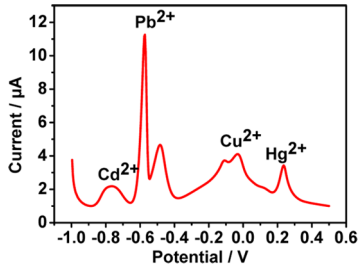


**Figure 4.** DPASVs for 0.8 μM each of $Cd^{2+}$, $Pb^{2+}$, $Cu^{2+}$, and $Hg^{2+}$ on Au nanoparticle modified GCE in 0.1 M acetate buffer. The conditions are respectively, pH 5.0, deposition potential −1.0 V, deposition time 300 s, detection temperature, 45 °C, amplitude 25 mV, increment potential 4 mV, frequency 15 Hz. The Ag/AgCl electrode was chosen as the counter electrode.

carried out for 300 s at −1.0 V in a solution containing 0.8 μM each of $Cd^{2+}$, $Pb^{2+}$, $Cu^{2+}$, and $Hg^{2+}$ in 0.1 M acetate buffer (pH 5.0), the sharp and high peak current for the four target metal ions were obtained. The increase in stripping currents at this modified electrode displayed that the AuNPs/GC electrode as working electrode is very suitable for the accumulation process of $Cd^{2+}$, $Pb^{2+}$, $Cu^{2+}$, and $Hg^{2+}$ on the electrode surface, and they can be identified at potentials of −0.78, −0.56, 0.00, and 0.25 V, respectively.

**3.3. Experimental Parameters Optimization.** In order to get maximum sensitivity for detecting heavy metal by using the AuNPs/GC electrode, the voltammetric parameters such as pH value, preconcentration potential, detection temperature, and preconcentration time were optimized. All the experiments were performed in mixed solution including 0.8 μM each of $Cd^{2+}$, $Pb^{2+}$, $Cu^{2+}$, and $Hg^{2+}$. To obtain the error analysis, several parallel samples were tested for several times under the same condition. From the detecting results, we obtained measuring errors range between 5% and 20%, which are marked by error bars on points in Figure 5.

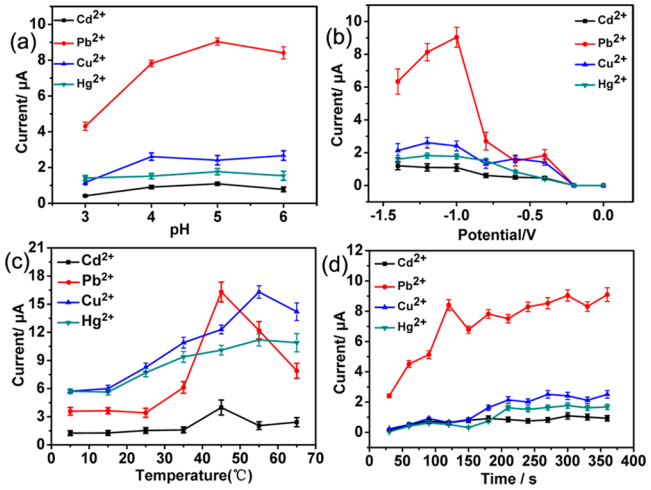


**Figure 5.** Experimental parameters optimization. Influence of (a) pH value; (b) preconcentration potential; (c) detection temperature; and (d) preconcentration time on the voltammetric response of the Au nanoparticle modified GCE. Data were obtained by DPASV for 0.8 μM each of $Cd^{2+}$, $Pb^{2+}$, $Cu^{2+}$, and $Hg^{2+}$. DPASV conditions are identical to those in Figure 4. The error bars are labeled on points.

*Solution pH.* The voltammetric behavior of the four metal ions was strongly influenced by the pH of the buffer solution, so the solution pH must be carefully considered. Figure 5a displayed the voltammetric behavior to the four target heavy metal ions at different pH value in acetate buffer supporting electrolyte. The effect of pH on the voltammetric response was researched in the range of 3.0 to 6.0 in 0.1 M acetate buffer solution. The anodic peak currents for $Cd^{2+}$, $Pb^{2+}$, and $Hg^{2+}$ were gradually increased as pH value was changed from 3.0 to 5.0. As the pH value was further increased to 6.0, for $Cd^{2+}$ and $Hg^{2+}$ the anodic peak current decreased slightly; in contrast, $Pb^{2+}$'s anodic peak current decreased distinctly. In general, the anodic peak currents for the four metal ions reached a optimization at pH 5.0.

When the pH value was too low, such as 3.0, the small response of AuNPs/GC electrode to four metal ions may be attributed to that the AuNPs on the electrode surface be disturbed by a large number of hydrogen ions ($H^+$) in the solution. With the increase of pH value, the sensitivity was improved due to low concentration of $H^+$. If pH value was too high, such as 6.0, some stripping signals began to decrease, which may be relative to hydrolysis or valence change of the four kinds of mental ions.[8] Therefore, pH value of 5.0 in 0.1 M acetate buffer solution should be an optimization for detecting the four heavy metal ions by the Au NPs/GC electrode.

*Preconcentration Potential.* In the stripping voltammetry analysis method, the application of preconcentration potential is very important to electrode sufficient accumulation and reduction. Thus, the effect of the deposition potential on the peak current after 300 s accumulation was investigated in the potential range from 0 to −1.4 V in 0.1 M acetate buffer solution at pH 5.0. The results are demonstrated in Figure 5b. It can be seen when the deposition potential shifts from 0 to −1.4 V, the stripping peak currents for $Cd^{2+}$, $Pb^{2+}$, and $Hg^{2+}$ reach the highest at −1.0 V. For $Cu^{2+}$, deposition potential was best at −1.2 V. The different metal ions' stripping peak currents may be due to different standard potentials. In our case, we select −1.0 V as the optimal preconcentration potential for the following detections.


dx.doi.org/10.1021/am404816e | ACS Appl. Mater. Interfaces 2014, 6, 65−71

*Solution Temperature.* The effect of solution temperature on the detection of the four heavy metal analysis in the range of 5−60 °C was investigated in our work. The initial temperature of solution was 5 °C. The changes of temperature were performed by directly heating the solution. The relationship between solution temperatures and peak currents of four target metal ions were shown in Figure 5c. As the solution temperature increases from 5 to 45 °C, $Cd^{2+}$ and $Hg^{2+}$' s peak currents increase gently and remained almost constant with the increase of temperature. $Pb^{2+}$ and $Cu^{2+}$' s peak currents reached a maximum at 45 and 35 °C respectively, and when the temperature went higher, the peak currents decreased. A solution temperature of 45 °C may be the most suitable temperature for metal ions' accumulation and reduction at the surface of the AuNPs/GC electrode. We choose 45 °C as the solution temperature for the following simultaneous detections. The solution temperature effects in these electrochemical anodic stripping voltammetry can be easily understood. The solution temperature affects the mobility of the ions in solution.[57] Relative to low temperature such as 5 °C, the warmer temperature is more beneficial to a faster movement of the metal ions to the working electrode surface. This can lead to a significant improvement of the sensitivity of the AuNPs/GC electrode during the heavy metal ions multidetection. Thus, as the temperature increase, the stripping peak currents of the four heavy metal ions are boosted. When up to a certain temperature (such as 45 °C for $Pb^{2+}$), the adsorption and desorption of the metal ions on the surface of the working electrode keep in balance and the peak currents reach the maximum. When the temperature was higher, sensitivity of the AuNPs/GC electrode reduced. Due to the optimized temperature, we need a temperature-controlled heating device in real applications.

*Preconcentration Time.* The preconcentration time is an important factor affecting the detection limit and the sensitivity. In stripping voltammetry, the increase of deposition time usually brings about the proportional raise of the peak currents. Figure 5D shows an illustration of peak currents as a function of deposition time varying from 30 to 360 s. Peak currents of $Cd^{2+}$, $Pb^{2+}$, $Cu^{2+}$, and $Hg^{2+}$ slowly increase as the extension of deposition time from 30 to 300 s. After 300 s, the peak currents of mostly heavy ions are tending toward stability. Therefore, 300 s was chosen as the optimum deposition time.

**3.4. Detection of $Cd^{2+}$, $Pb^{2+}$, $Cu^{2+}$, and $Hg^{2+}$ Simultaneously under Optimized Conditions.** Using the optimal detecting conditions described above, the DPASVs of AuNPs/GC electrode in 0.1 M acetate buffer solution containing $Cd^{2+}$, $Pb^{2+}$, $Cu^{2+}$, and $Hg^{2+}$ ions with different concentrations are presented in Figure 6. From bottom to top, the increasing concentrations of heavy metal ions are 0, 0.3, 0.5, 0.6, 0.7, 0.8, 1.1, and 1.4 $\mu$M in sequence. There is no obvious signal obtained in NaAc−HAc solution (black dot line). In other curves, the DPASVs exhibited four peak currents at −0.78, −0.56, 0.00, and 0.25 V, which are corresponding to oxidation potential of Cd(0), Pb(0), Cu(0), and Hg(0), respectively. The corresponding linear calibration plots for peak currents of the four heavy metal ions were shown in Figure 7. The occasionally reverse phenomena (a peak height decrease with increasing metal ions concentration) are probably due to the interference effect from other metals. And likewise, we did same measurements repeatedly to get the experiment error, and we obtained the results with error range from 5% to 15%, as labeled by error bars on points in Figure7. The

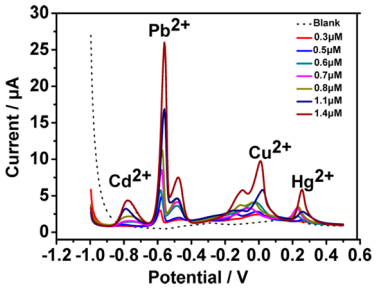


**Figure 6.** DPASV response of the AuNPs/GC electrode for the simultaneous detection of $Cd^{2+}$, $Pb^{2+}$, $Cu^{2+}$, and $Hg^{2+}$ over a concentration range of 0 to 1.4 $\mu$M for each metal ion. From bottom to top, 0, 0.3, 0.5, 0.6, 0.7, 0.8, 1.1, and 1.4 $\mu$M. The detection was carried out under the optimal detecting conditions.

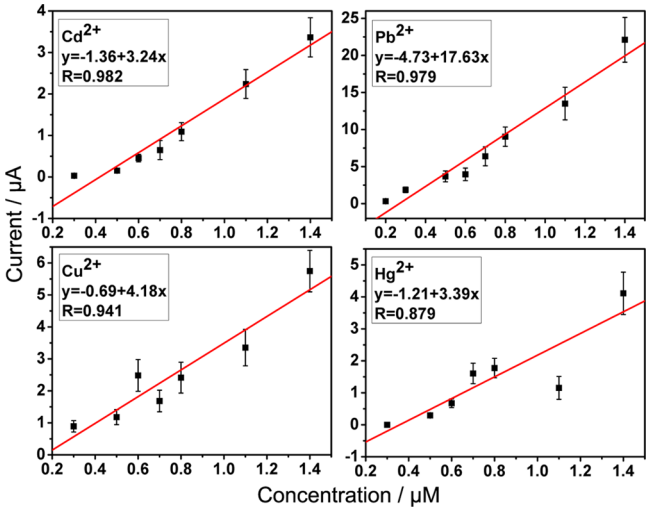


**Figure 7.** Respective calibration plots of $Cd^{2+}$, $Pb^{2+}$, $Cu^{2+}$, and $Hg^{2+}$ corresponding to Figure 6. The error bars are labeled on points.

linearization equations were obtained by fitting and expressed as follows: $i/\mu A = -1.36 + 3.24c/\mu M$, $i/\mu A = -4.73 + 17.63c/\mu M$, $i/\mu A = -0.69 + 4.18c/\mu M$, $i/\mu A = -1.21 + 3.39c/\mu M$, for $Cd^{2+}$, $Pb^{2+}$, $Cu^{2+}$, and $Hg^{2+}$, respectively. The results shows that we can detect $Cd^{2+}$, $Pb^{2+}$, $Cu^{2+}$, and $Hg^{2+}$ simultaneously with a low concentration of $3 \times 10^{-7}$ M in the experiments.

Although the electrochemical sensing property of the AuNPs/GC electrode to heavy metal ions was not the best comparing to some working electrodes reported previously, the gold nanoparticles prepared by laser ablation in liquid were first applied to electrochemical working electrode to simultaneously detecting four heavy metal ions, and the obtained sensing performance is good enough for practical application. Such an attractive electroanalytical performance of the AuNPs/GC electrode may contribute to four reasons. First, the gold nanoparticles have very good conductivity and correspondingly high current density.[58] Second, the gold nanoparticles have clean and bare surface because of preparing in deionized water without any chemical additives. These two aspects are all quite conducive to increasing the electron transfer rate between metal ions and electrode. Third, the gold nanoparticles possess higher electrochemical activity compared to nanoparticles by other means due to high concentration of defect produced during the nonequilibrium process.[45] Finally, the gold nanoparticles fabricated by LAL are small, so there are large available surface areas of the working electrode for the metals ions'


dx.doi.org/10.1021/am404816e | ACS Appl. Mater. Interfaces 2014, 6, 65−71

deposition to exhibit well-separated stripping signals of each metal.

## CONCLUSION

In conclusion, gold nanoparticles were prepared by LAL method, and used for the simultaneous electrochemical determination of $Cd^{2+}$, $Pb^{2+}$, $Cu^{2+}$, and $Hg^{2+}$ for the first time. Through optimizing the electrochemical detection conditions, we can detect $Cd^{2+}$, $Pb^{2+}$, $Cu^{2+}$, and $Hg^{2+}$ simultaneously with a concentration of $3 \times 10^{-7}$ M in the experiments. In general, the gold nanoparticles obtained by LAL method may be promising candidates for use in probing trace heavy metal ions due to its high electrical conductivity, wide potential window, clean and nontoxicity. This work can give important references in the field of both LAL and electrochemical detection. Also, it should be mentioned that much deeper work is needed to improve the application level, such as detection limits in the experiments.

## ASSOCIATED CONTENT

### Supporting Information

FESEM images, DPASVs curves, and the cyclic voltammetric curves. This information is available free of charge via the Internet at http://pubs.acs.org/.

## AUTHOR INFORMATION

### Corresponding Authors

*E-mail: duangt@issp.ac.cn.

*E-mail: wpcai@issp.ac.cn.

### Notes

The authors declare no competing financial interest.

## ACKNOWLEDGMENTS

The authors acknowledge the financial supports from the National Basic Research Program of China (973 Program, Grant No. 2011CB302103), Natural Science Foundation of China (Grant No. 11174286 and 11374303), and provincial Natural Science Foundation of Anhui (Grant No. 11040606M62).

## REFERENCES

(1) Wiener, J. G.; Krabbenhoft, D. P.; Heinz, G. H.; Scheuhammer, A. M. In *Handbook of Ecotoxicology*; Hoffman, D. J., Ed.; CRC Press LLC: Boca Rato, FL, 2003; p 409.
(2) Darwish, I. A.; Blake, D. A. *Anal. Chem.* **2001**, *74*, 52−58.
(3) Hwang, T. J.; Jiang, S. J. *J. Anal. At. Spectrom.* **1996**, *11*, 353−357.
(4) Wan, Z.; Xu, Z.; Wang, J. *Analyst* **2006**, *131*, 141−147.
(5) Kim, Y. J.; Johnson, R. C.; Hupp, J. T. *Nano Lett.* **2001**, *1*, 165−167.
(6) Liu, H. W.; Jiang, S. J.; Liu, S. H. *Spectrochim. Acta Part B: At. Spectrosc.* **1999**, *54*, 1367−1375.
(7) Rahman, M. R.; Okajima, T.; Ohsaka, T. *Anal. Chem.* **2010**, *82*, 9169−9176.
(8) Wei, Y.; Gao, C.; Meng, F. L.; Li, H. H.; Wang, L.; Liu, J. H.; Huang, X. J. *J. Phys. Chem. C* **2012**, *116*, 1034−1041.
(9) Yu, X. Y.; Luo, T.; Jia, Y.; Xu, R. X.; Gao, C.; Zhang, Y. X.; Liu, J. H.; Huang, X. J. *Nanoscale* **2012**, *4*, 3466−3474.
(10) Limon-Petersen, J. G.; Streeter, I.; Rees, N. V.; Compton, R. G. *J. Phys. Chem. C* **2008**, *112*, 17175−17182.
(11) Dai, X.; Nekrassova, O.; Hyde, M. E.; Compton, R. G. *Anal. Chem.* **2004**, *76*, 5924−5929.
(12) Jena, B. K.; Raj, C. R. *Anal. Chem.* **2008**, *80*, 4836−4844.
(13) Li, M.; Li, D. W.; Li, Y. T.; Xu, D. K.; Long, Y. T. *Anal. Chim. Acta* **2011**, *701*, 157−163.
(14) Yoon, J. H.; Yang, J.; Kim, J.; Bae, J.; Shim, Y. B.; Won, M. S. *Bull. Korean Chem. Soc.* **2010**, *31*, 140−145.
(15) El Tall, O.; Renault, N. J.; Sigaud, M.; Vittori, O. *Electroanalysis* **2007**, *19*, 1152−1159.
(16) Forsberg, G.; O'Laughlin, J. W.; Megargle, R. G.; Koirtyihann, S. R. *Anal. Chem.* **1975**, *47*, 1586−1592.
(17) Cesarino, I.; Cavalheiro, É. T. G.; Brett, C. M. A. *Electroanalysis* **2010**, *22*, 61−68.
(18) van Staden, J. F.; Matoetoe, M. C. *Anal. Chim. Acta* **2000**, *411*, 201−207.
(19) Rashid, M. H.; Bhattacharjee, R. R.; Kotal, A.; Mandal, T. K. *Langmuir* **2006**, *22*, 7141−7143.
(20) Song, W.; Zhang, L.; Shi, L.; Li, D. W.; Li, Y.; Long, Y. T. *Microchim. Acta* **2010**, *169*, 321−326.
(21) Barry, R. C.; Lin, Y.; Wang, J.; Liu, G.; Timchalk, C. A. *J. Expo. Sci. Environ. Epidemiol.* **2008**, *19*, 1−18.
(22) Pumera, M.; Ambrosi, A.; Bonanni, A.; Chng, E. L. K.; Poh, H. L. *TrAC Trends Anal. Chem.* **2010**, *29*, 954−965.
(23) Hwang, G. H.; Han, W. K.; Park, J. S.; Kang, S. G. *Talanta* **2008**, *76*, 301−308.
(24) Xu, H.; Zeng, L.; Xing, S.; Xian, Y.; Shi, G.; Jin, L. *Electroanalysis* **2008**, *20*, 2655−2662.
(25) Yantasee, W.; Charnhattakorn, B.; Fryxell, G. E.; Lin, Y.; Timchalk, H. C.; Addleman, R. S. *Anal. Chim. Acta* **2008**, *620*, 55−63.
(26) Renedo, O. D.; Julia Arcos Martínez, M. *Electrochem. Commun.* **2007**, *9*, 820−826.
(27) Toghill, K. E.; Xiao, L.; Wildgoose, G. G.; Compton, R. G. *Electroanalysis* **2009**, *21*, 1113−1118.
(28) Saha, K.; Agasti, S. S.; Kim, C.; Li, X.; Rotello, V. M. *Chem. Rev.* **2012**, *112*, 2739−2779.
(29) Majid, E.; Hrapovic, S.; Liu, Y.; Male, K. B.; Luong, J. H. T. *Anal. Chem.* **2005**, *78*, 762−769.
(30) Daniel, M. C.; Astru, D. *Chem. Rev.* **2004**, *104*, 293.
(31) Zeng, H. B.; Cai, W. P.; Li, Y.; Hu, J. L.; Liu, P. S. *J. Phys. Chem. B* **2005**, *109*, 18260−18266.
(32) He, H.; Cai, W. P.; Lin, Y. X.; Chen, B. S. *Chem. Commun.* **2010**, *46*, 7223−7225.
(33) Yang, S. K.; Cai, W. P.; Liu, G. Q.; Zeng, H. B. *J. Phys. Chem. C* **2009**, *113*, 7692−7696.
(34) He, H.; Cai, W. P.; Lin, Y. X.; Chen, B. S. *Langmuir* **2010**, *26*, 8925−8932.
(35) Zeng, H. B.; Du, X. W.; Singh, S. C.; Kulinich, S. A.; Yang, S. K.; He, J.; Cai, W. P. *Adv. Funct. Mater.* **2012**, *22*, 1333−1353.
(36) Mafune, F.; Kohno, J.; Takeda, Y.; Kondow, T.; Sawabe, H. *J. Phys. Chem. B* **2001**, *105*, 5114−5120.
(37) Procházka, M.; Mojzeš, P.; Štěpánek, J.; Vlčková, B.; Turpin, P. Y. *Anal. Chem.* **1997**, *69*, 5103−5108.
(38) Mafune, F.; Kohno, J. Y.; Takeda, Y.; Kondow, T. *J. Phys. Chem. B* **2003**, *107*, 4218−4223.
(39) Tilaki, R. M.; Irajizad, A.; Mahdavi, S. M. *Appl. Phys. A: Mater. Sci. Process.* **2007**, *88*, 415−419.
(40) Chen, G. X.; Hong, M. H.; Lan, B.; Wang, Z. B.; Lu, Y. F.; Chong, T. C. *Appl. Surf. Sci.* **2004**, *228*, 169−175.
(41) Simakin, A. V.; Voronov, V. V.; Shafeev, G. A.; Brayner, R.; Bozon-Verduraz, F. *Chem. Phys. Lett.* **2001**, *348*, 182−186.
(42) Saitow, K. I. *J. Phys. Chem. B* **2005**, *109*, 3731−3733.
(43) Liang, C. H.; Shimizu, Y.; Masuda, M.; Sasaki, T.; Koshizaki, N. *Chem. Mater.* **2004**, *16*, 963−965.
(44) Liu, P. S.; Cai, W. P.; Zeng, H. B. *J. Phys. Chem. C* **2008**, *112*, 3261−3266.
(45) Anikin, K. V.; Melnik, N. N.; Simakin, A. V.; Shafeev, G. A.; Voronov, V. V.; Vitukhnovsky, A. G. *Chem. Phys. Lett.* **2002**, *366*, 357−360.
(46) Zeng, H. B.; Duan, G. T.; Li, Y.; Yang, S. K.; Xu, X. X.; Cai, W. P. *Adv. Funct. Mater.* **2010**, *20*, 561−572.
(47) Liu, P.; Wang, C. X.; Chen, X. Y.; Yang, G. W. *J. Phys. Chem. C* **2008**, *112*, 13450−13456.
(48) Liu, P.; Cao, Y. L.; Cui, H.; Chen, X. Y.; Yang, G. W. *Cryst. Growth Des.* **2008**, *8*, 559−563.

(49) Liu, P.; Cao, Y. L.; Wang, C. X.; Chen, X. Y.; Yang, G. W. *Nano Lett.* **2008**, *8*, 2570−2575.
(50) Wang, J. B.; Yang, G. W.; Zhang, C. Y.; Zhong, X. L.; Ren, Z. H. A. *Chem. Phys. Lett.* **2003**, *367*, 10−14.
(51) Citroni, M.; Ceppatelli, M.; Bini, R.; Schettino, V. *Science* **2002**, *15*, 2058.
(52) Liu, Q. X.; Yang, G. W.; Zhang, J. X. *Chem. Phys. Lett.* **2003**, *373*, 57−61.
(53) Zeng, H. B.; Li, Z. G.; Cai, W. P.; Cao, B. Q.; Liu, P. S.; Yang, S. K. *J. Phys. Chem. B* **2007**, *111*, 14311−14317.
(54) Campbell, F.; Belding, S.; Baron, R.; Xiao, L.; Compton, R. *J. Phys. Chem.C* **2009**, *113*, 9053−9062.
(55) Finot, O.; Braybrook, D.; McDermott, T. *J. Electroanal. Chem.* **1999**, *466*, 234−241.
(56) Kozlowska, A.; Conway, E.; Hamelin, A.; Stoicovicu, L. *J. Electroanal. Chem.* **1987**, *228*, 429−453.
(57) Aragay, G.; Pons, J.; Merkoci, A. *J. Mater. Chem.* **2011**, *21*, 4326−4331.
(58) Streeter, I.; Baron, R.; Compton, R. G. *J. Phys. Chem. C* **2007**, *111*, 17008−17014.